Comparing Social Distancing, Lockdown, and Vaccination: A Study Based on a Generalised SEIR-Type Epidemic Model

Jonathan Hoseana and Daniel Salim

***Abstract*—We construct a generalisation of a recently proposed SEIR-type epidemic model involving social distancing and lockdown intensities, by incorporating the proportion of vaccinated newborns and replacing the bilinear incidence rate with a Holling type II incidence rate. We establish the dynamical properties of the resulting model: the solutions' non-negativity and boundedness, the equilibria and basic reproduction number, as well as the local asymptotic stability of the equilibria. Subsequently, we use the forward Euler method to construct a discrete version of the model, which admits the same equilibria. We formulate sufficient conditions for the local asymptotic stability of these equilibria, involving not only the basic reproduction number but also the discretisation step size. Finally, using two sets of parameter values representing disease-free and endemic situations, we conduct numerical simulations and sensitivity analysis, the latter revealing that vaccination is more effective for preventing an outbreak in a disease-free situation, whereas social distancing and lockdown are more effective for resolving an endemic situation and lowering the epidemic peak.**

***Index Terms*—social distancing, lockdown, vaccination, Holling type II, basic reproduction number, forward Euler method, sensitivity analysis, epidemic peak**

I. Introduction

THE recent COVID-19 pandemic has led to a remarkable surge of interest in disease-transmission modelling. Indeed, mathematical models have been developed to understand not only how the disease itself is transmitted within a certain population, but also to investigate whether eradicative interventions such as social distancings and lockdowns could effectively mitigate the transmission. For the latter purpose, classical disease-transmission models such as the Kermack-McKendrick SIR-type model [38], albeit remaining of extensive use [8], [9], [25], [37], [47], [68], [22], [40], often prove insufficient. As a result, through modifications and alignments with real-world observations, more complex mathematical models have been proposed, and employed to better assess the impact of such interventions [3], [10], [12], [16], [29], [31], [57], [63], [70], [54], [42], [14], [33], [1], [26], [55]. Additionally, disease-transmission models have also been used to study the propagation of alcoholism [41], [20], [64], computer virus [74], [75], game addiction [58], and public opinion [66], [67].

In 2022, Al-Harbi and Al-Tuwairqi [3] proposed a four-compartment disease-transmission model of type SEIR, with the aim of modelling the transmission of COVID-19 in Saudi Arabia, thereby complementing previous studies on COVID-19 in the same country [2], [5], [6], [7], [13]. A distinctive feature of their model lies in the incorporation of two percentage-valued parameters representing social distancing and lockdown intensities. Using the model, the authors derived an expression for the disease's basic reproduction number in terms of the involved parameters, demonstrated the existence of two equilibria: disease-free and endemic, and established the equilibria's global asymptotic stability. The authors also fitted their model to the actual 2020 data provided by the Saudi Ministry of Health, using the results to conduct numerical experiments and sensitivity analysis of the basic reproduction number. The latter revealed that the social distancing and lockdown intensities are indeed parameters upon which the basic reproduction number depends particularly sensitively.

The SEIR-type model of Al-Harbi and Al-Tuwairqi, however, does not take into account another intervention strategy whose effectiveness has been confirmed by numerous studies [17], [30], [44], [46], [60], [61], [70]: vaccination. Indeed, the practice of incorporating vaccination into disease-transmission models has been in place for a significant period. The variable-population Kermack-McKendrick SIR-type model enhanced with constant vaccination, discussed in various resources [45], [48], [60], has been a popular prototypical disease-transmission model which takes into account vaccination. In this paper, we enhance the model of Al-Harbi and Al-Tuwairqi by adopting the same idea. That is, we introduce a new percentage-valued parameter representing the proportion of vaccinated newborns, so that only unvaccinated newborns are assumed to be susceptible. Later we shall reconduct a sensitivity analysis to compare the significance of this parameter with that of social distancing and lockdown intensities.

In addition, the model of Al-Harbi and Al-Tuwairqi, as also the model of Kermack and McKendrick, employs the so-called bilinear form of incidence rate. This means that, at any given time, the rate at which susceptible individuals become infectious is assumed to be proportional to the product of the number of susceptible and infected individuals. Such an assumption leads to a property which is not entirely realistic, namely that the incidence rate becomes arbitrarily large as the number of infected individuals increases. In reality, large numbers of infected individuals may serve as noticeable warnings to susceptible individuals, prompting them to adjust their behaviour to reduce transmission. A generalisation of the bilinear incidence rate which captures such a behaviour adjustment is the so-called Holling type II incidence rate

Manuscript received May 1, 2025; revised June 26, 2025.

Jonathan Hoseana is a researcher at the Center for Mathematics and Society, Faculty of Science, Parahyangan Catholic University, Bandung, Indonesia (corresponding author, e-mail: j.hoseana@unpar.ac.id).

Daniel Salim is a researcher at the Center for Mathematics and Society, Faculty of Science, Parahyangan Catholic University, Bandung, Indonesia (e-mail: daniel.salim@unpar.ac.id).

[15], [35], [59], [36], [73]. Unlike the bilinear incidence rate which involves only a single parameter: the incidence coefficient, the Holling type II incidence rate involves two parameters: the incidence and the inhibition coefficients, the latter quantifying the intensity of the mentioned behaviour adjustment.

In the upcoming section II, we thus modify the SEIR-type disease-transmission model of Al-Harbi and Al-Tuwairqi by incorporating the vaccination proportion and replacing the bilinear incidence rate with a Holling type II incidence rate. We establish the non-negativity and boundedness of the solutions of the resulting model, determine the model's equilibria and basic reproduction number, and relate the local asymptotic stability of each equilibrium to the value of the basic reproduction number. In the subsequent section III, we discretise our model using the forward Euler method, deduce that the resulting discrete model possesses the same equilibria, and formulate criteria for the local asymptotic stability of these equilibria, which involve not only the basic reproduction number but also the discretisation step size. In section IV, we conduct numerical simulations using two sets of parameter values derived from the work of Al-Harbi and Al-Tuwairqi [3], representing two qualitatively different cases: a disease-free case and an endemic case. In the former case, we analyse the sensitivity of the basic reproduction number with respect to the model's parameters, using the results to compare the effectiveness of social distancing, lockdown, and vaccination for preserving the disease-free state. In the latter case, we analyse the sensitivity of not only the basic reproduction number but also the epidemic peak with respect to the model's parameters, using the results to compare the effectiveness of social distancing, lockdown, and vaccination for eradicating the disease and lowering the epidemic peak. In the final section V, we state our conclusions and describe avenues for further research.

II. Model construction and analysis

In this section, we first construct a modification of the SEIR-type disease-transmission model of Al-Harbi and Al-Tuwairqi [3] which takes into account vaccination and employs the Holling type II form of incidence rate (subsection II-A). Subsequently, we verify the model's biological feasibility, establishing its solutions' non-negativity and boundedness (subsection II-B). Finally, we analyse the model from the perspective of dynamical systems theory [4], [48], [56], [62], determining its equilibria and basic reproduction number (subsection II-C) as well as conditions for the local asymptotic stability of each equilibria in terms of the basic reproduction number (subsection II-D).

A. Model construction

To begin our model construction, let us consider a population over which a disease spreads, which is divided into four compartments comprising those of susceptible, exposed, infected, and recovered individuals, respectively. We assume that a proportion of $v \in [0,1]$ of newborns are vaccinated, and that only unvaccinated newborns enter the population, specifically the susceptible compartment. Assuming a birth rate of $\eta \geqslant 0$ individuals per day, this means that $(1-v)\,\eta$ individuals per day enter the susceptible compartment. Next, employing a Holling type II form of incidence rate, $\beta SI/(1+\alpha I)$ individuals per day, where $\beta > 0$ and $\alpha \geqslant 0$ denote, respectively, the incidence and inhibition coefficients, and combining this with the lockdown intensity $1-\rho \in (0,1)$ and social-distancing intensity $\mathrm{SD} = 1-\tau$, where $\tau \in (0,1)$, we assume that susceptible individuals become exposed at the rate of $\rho\tau\beta SI/(1+\alpha I)$ individuals per day. Furthermore, letting the disease's incubation and recovery coefficients be $\gamma > 0$ per day and $\delta > 0$ per day, respectively, we assume that exposed individuals become infected at the rate of γE individuals per day, and infected individuals become recovered at the rate of δI individuals per day. Finally, letting the natural and disease-caused death coefficients be $\mu > 0$ per day and $d > 0$ per day, respectively, we assume that the numbers of susceptible, exposed, and recovered individuals decrease due to deaths at the rates of μS, μE, and μR, respectively, while the numbers of infected individuals decreases due to deaths at the rate of $(d+\mu)\,I$.

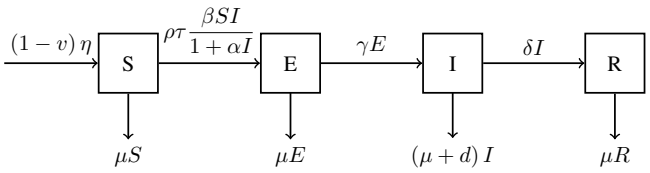

Fig. 1. The compartment diagram of our SEIR-type model (1).

The above assumptions lead to the compartment diagram shown in Figure 1, and the system of differential equations

$$\begin{cases} \dfrac{\mathrm{d}S}{\mathrm{d}t} &= (1-v)\,\eta - \rho\tau\dfrac{\beta SI}{1+\alpha I} - \mu S, \\ \dfrac{\mathrm{d}E}{\mathrm{d}t} &= \rho\tau\dfrac{\beta SI}{1+\alpha I} - (\gamma+\mu)\,E, \\ \dfrac{\mathrm{d}I}{\mathrm{d}t} &= \gamma E - (\delta+d+\mu)\,I, \\ \dfrac{\mathrm{d}R}{\mathrm{d}t} &= \delta I - \mu R. \end{cases} \tag{1}$$

Notice that by setting $v = \alpha = 0$, we retrieve the original model of Al-Harbi and Al-Tuwairqi [3, eqn. (1)]. Thus, the model (1) can be regarded as a generalisation of the model of Al-Harbi and Al-Tuwairqi. The parameters involved in the model (1), along with their values to be used in our numerical simulations (section IV), are summarised in Table I.

B. Non-negativity and boundedness of solutions

Let us now verify that the model (1) is biologically feasible, particularly that the numbers of susceptible, exposed, infected, and recovered individuals as governed by the model remain non-negative at all times, provided that their initial values are non-negative. For this purpose, let $\mathbb{R}_+ = [0,\infty)$, and let

$$(S,E,I,R) = (S(t),E(t),I(t),R(t)) \tag{2}$$

be a solution of the model (1) associated to an initial condition $(S(0),E(0),I(0),R(0)) \in \mathbb{R}_+^4$.

By the model's equations, we have that if $S(t_1) = 0$ for some $t_1 \geqslant 0$, then

$$\left.\frac{\mathrm{d}S}{\mathrm{d}t}\right|_{t=t_1} = (1-v)\,\eta > 0.$$

TABLE I
PARAMETERS USED IN OUR MODEL AND THEIR VALUES SELECTED FOR OUR NUMERICAL SIMULATIONS (SECTION IV).

Parameter	Description	Unit	Value for simulation	Source
v	vaccination proportion	–	0.8 0.1	simulated
η	birth rate	individual/day	1250	[3, Tbl. 1]
$1-\rho$	lockdown intensity	–	0.1	simulated
$1-\tau$	social-distancing intensity	–	0.5	simulated
β	incidence coefficient	1/(individual×day)	$1.0063 \cdot 10^{-4}$	[3, Tbl. 1]
α	incidence inhibition coefficient	1/individual	10^{-4}	simulated
μ	natural death coefficient	1/day	0.04	[3, Tbl. 1]
d	death-by-disease coefficient	1/day	$2.3724 \cdot 10^{-1}$	[3, Tbl. 1]
γ	incubation coefficient	1/day	0.167	[3, Tbl. 1]
δ	recovery coefficient	1/day	$3.2772 \cdot 10^{-1}$	[3, Tbl. 1]
$S(0)$	initial number of susceptible individuals	individual	2999	simulated
$E(0)$	initial number of exposed individuals	individual	1	simulated
$I(0)$	initial number of infected individuals	individual	0	simulated
$R(0)$	initial number of recovered individuals	individual	0	simulated

This implies that for every $t \geqslant 0$ we have $S(t) \in \mathbb{R}_+$. Next, suppose that for some $t_2 \geqslant 0$ and $t_3 \geqslant 0$ we have

$$(E(t_2), I(t_2)) = (0, I(t_2)) \in \mathbb{R}_+^2$$

and

$$(E(t_3), I(t_3)) = (E(t_3), 0) \in \mathbb{R}_+^2.$$

If $t_2 \neq t_3$, then for $\Delta t \in [0, 1/(\delta + d + \mu))$ we have

$$E(t_2 + \Delta t) = \rho\tau \frac{\beta S(t_2) I(t_2)}{1 + \alpha I(t_2)} \Delta t + \mathcal{O}\left((\Delta t)^2\right), \quad (3)$$

$$I(t_2 + \Delta t) = [1 - (\delta + d + \mu)\Delta t] I(t_2) + \mathcal{O}\left((\Delta t)^2\right), \quad (4)$$

and for $\Delta t \in [0, 1/(\gamma + \mu))$ we have

$$E(t_3 + \Delta t) = [1 - (\gamma + \mu)\Delta t] E(t_3) + \mathcal{O}\left((\Delta t)^2\right), \quad (5)$$

$$I(t_3 + \Delta t) = \gamma E(t_3) \Delta t + \mathcal{O}\left((\Delta t)^2\right), \quad (6)$$

where the terms preceding $\mathcal{O}\left((\Delta t)^2\right)$ on the right-hand sides of (3), (4), (5), and (6) are positive. On the other hand, if $t_2 = t_3$, then

$$\left.\frac{\mathrm{d}^n E}{\mathrm{d}t^n}\right|_{t=t_2} = \left.\frac{\mathrm{d}^n I}{\mathrm{d}t^n}\right|_{t=t_3} = 0 \qquad \text{for every } n \in \mathbb{N}.$$

Consequently, for sufficiently small $\Delta t > 0$ we have $E(t_2 + \Delta t) = I(t_3 + \Delta t) = 0$. It follows that for every $t \geqslant 0$ we have $(E(t), I(t)) \in \mathbb{R}_+^2$.

Finally, if $R(t_4) = 0$ for some $t_4 \geqslant 0$, then, using the fact that $I(t) \in \mathbb{R}_+$ for every $t \geqslant 0$, we have

$$\left.\frac{\mathrm{d}R}{\mathrm{d}t}\right|_{t=t_4} = \delta I(t_4) \geqslant 0.$$

In the case $I(t_4) = 0$, we have

$$\left.\frac{\mathrm{d}^2 R}{\mathrm{d}t^2}\right|_{t=t_4} = \delta\gamma E(t_4) \geqslant 0.$$

In the case $E(t_4) = 0$, we have

$$\left.\frac{\mathrm{d}^n R}{\mathrm{d}t^n}\right|_{t=t_4} = 0 \qquad \text{for every } n \in \mathbb{N}.$$

Thus, for every $t \geqslant 0$ we have $R(t) \in \mathbb{R}_+$. This proves that the solution (2) remains in $\mathbb{R}_+^4$ for every $t \geqslant 0$.

Next, letting $N = N(t) = S(t) + E(t) + I(t) + R(t)$ for every $t \geqslant 0$ and adding the four equations in (1), we obtain the following which shows that our total population is not constant:

$$\frac{\mathrm{d}N}{\mathrm{d}t} = (1 - v)\eta - \mu N - dI \leqslant (1 - v)\eta - \mu N.$$

Multiplying both sides by $\mathrm{e}^{\mu t}$ gives

$$\frac{\mathrm{d}}{\mathrm{d}t}\left[\mathrm{e}^{\mu t} N(t)\right] \leqslant \frac{\mathrm{d}}{\mathrm{d}t}\left[\frac{(1 - v)\eta}{\mu}\mathrm{e}^{\mu t} + N(0) - \frac{(1 - v)\eta}{\mu}\right].$$

The functions $\mathrm{e}^{\mu t} N(t)$ and $(1 - v)\eta\,\mathrm{e}^{\mu t}/\mu + N(0) - (1 - v)\eta/\mu$ both evaluate to $N(0)$ at $t = 0$ and, by the above inequality, at every $t \geqslant 0$, the slope of the former function is bounded above by that of the latter function. This implies that for every $t \geqslant 0$ we have

$$\mathrm{e}^{\mu t} N(t) \leqslant \frac{(1 - v)\eta}{\mu}\mathrm{e}^{\mu t} + N(0) - \frac{(1 - v)\eta}{\mu}.$$

Multiplying both sides by $\mathrm{e}^{-\mu t}$ gives

$$\begin{aligned} N(t) &\leqslant \frac{(1 - v)\eta}{\mu} + \left[N(0) - \frac{(1 - v)\eta}{\mu}\right]\mathrm{e}^{-\mu t} \\ &\leqslant \max\left\{N(0), \frac{(1 - v)\eta}{\mu}\right\}. \end{aligned} \quad (7)$$

On the other hand, we have that

$$\begin{aligned} \frac{\mathrm{d}N}{\mathrm{d}t} &= (1 - v)\eta + d(S + E + R) - (\mu + d)N \\ &\geqslant (1 - v)\eta - (\mu + d)N. \end{aligned}$$

Multiplying both sides by $\mathrm{e}^{(\mu+d)t}$ gives

$$\frac{\mathrm{d}}{\mathrm{d}t}\left[\mathrm{e}^{(\mu+d)t} N(t)\right] \geqslant \frac{\mathrm{d}}{\mathrm{d}t}\left[\frac{(1 - v)\eta}{\mu + d}\mathrm{e}^{(\mu+d)t} + N(0) - \frac{(1 - v)\eta}{\mu + d}\right].$$

As before, the functions $\mathrm{e}^{(\mu+d)t} N(t)$ and $(1 - v)\eta\,\mathrm{e}^{(\mu+d)t}/(\mu + d) + N(0) - (1 - v)\eta/(\mu + d)$ both evaluate to $N(0)$ at $t = 0$ and, by the above inequality, at every $t \geqslant 0$, the slope of the former function is bounded below by that of the latter function. This implies that for every $t \geqslant 0$ we have

$$\mathrm{e}^{(\mu+d)t} N(t) \geqslant \frac{(1 - v)\eta}{\mu + d}\mathrm{e}^{(\mu+d)t} + N(0) - \frac{(1 - v)\eta}{\mu + d}.$$

Multiplying both sides by $\mathrm{e}^{-(\mu+d)t}$ gives

$$\frac{(1-v)\,\eta}{\mu+d}+\left[N(0)-\frac{(1-v)\eta}{\mu+d}\right]\mathrm{e}^{-(\mu+d)t} \geqslant \min\left\{N(0),\frac{(1-v)\,\eta}{\mu+d}\right\}. \tag{8}$$

From (7) and (8), we also have

$$\frac{(1-v)\,\eta}{\mu+d}\leqslant\lim_{t\to\infty}N(t)\leqslant\frac{(1-v)\,\eta}{\mu}.$$

We have thus established the following theorem.

Theorem 1. The set $\mathbb{R}^4_+$ is positively invariant under the model (1). Moreover, every solution $(S,E,I,R)=(S(t),E(t),I(t),R(t))$ of the model (1) associated to an initial condition $(S(0),E(0),I(0),R(0))\in\mathbb{R}^4_+$ satisfies

$$\min\left\{N(0),\frac{(1-v)\,\eta}{\mu+d}\right\}\leqslant S(t)+E(t)+I(t)+R(t)\leqslant\max\left\{N(0),\frac{(1-v)\,\eta}{\mu}\right\}$$

for every $t\geqslant 0$, where $N(0)=S(0)+E(0)+I(0)+R(0)$.

C. Equilibria and basic reproduction number

Let us next determine the equilibria of the model (1), which are the solutions of the system

$$\begin{cases}(1-v)\,\eta-\rho\tau\dfrac{\beta SI}{1+\alpha I}-\mu S=0,\\ \rho\tau\dfrac{\beta SI}{1+\alpha I}-(\gamma+\mu)\,E=0,\\ \gamma E-(\delta+d+\mu)\,I=0,\\ \delta I-\mu R=0.\end{cases} \tag{9}$$

The system's second equation gives

$$E=\frac{\rho\tau\beta SI}{(1+\alpha I)\,(\gamma+\mu)}. \tag{10}$$

Substituting this into the system's third equation gives

$$0=\gamma\frac{\rho\tau\beta SI}{(1+\alpha I)\,(\gamma+\mu)}-(\delta+d+\mu)\,I =I\left[\frac{\rho\tau\beta S}{(1+\alpha I)\,(\gamma+\mu)}-(\delta+d+\mu)\right],$$

which implies that either $I=0$ or

$$S=\frac{(\gamma+\mu)\,(\delta+d+\mu)\,(1+\alpha I)}{\beta\gamma\rho\tau}. \tag{11}$$

If $I=0$, then (10) gives $E=0$, the system's fourth equation gives $R=0$, and the system's first equation gives $S=(1-v)\,\eta/\mu$. Therefore,

$$\mathcal{E}_0=(S_0,E_0,I_0,R_0)=\left(\frac{(1-v)\eta}{\mu},0,0,0\right). \tag{12}$$

is the model's disease-free equilibrium.

Next, suppose that $I\neq 0$. Substituting (11) into the system's first equation gives

$$0=(1-v)\,\eta-\rho\tau\frac{\beta I}{1+\alpha I}\left[\frac{(\gamma+\mu)\,(\delta+d+\mu)\,(1+\alpha I)}{\beta\gamma\rho\tau}\right] =(1-v)\,\eta-\frac{(\gamma+\mu)\,(\delta+d+\mu)\,I}{\gamma} -\frac{\mu\,(\delta+\mu)\,(\delta+d+\mu)\,(1+\alpha I)}{\beta\gamma\rho\tau},$$

i.e.,

$$(1-v)\,\eta=\frac{(\gamma+\mu)\,(\gamma+d+\mu)}{\gamma}\left[I+\frac{\mu\,(1+\alpha I)}{\beta\rho\tau}\right].$$

Multiplying both sides by $\beta\gamma\rho\tau/\left[\mu\,(\gamma+\mu)\,(\delta+d+\mu)\right]$ gives

$$\frac{\eta\beta\gamma\tau\rho\,(1-v)}{\mu\,(\gamma+\mu)\,(\delta+d+\mu)}=\left(\frac{\beta\tau}{\mu}+\alpha\right)I+1,$$

from which one obtains

$$I=\frac{\mu}{\alpha\mu+\beta\rho\tau}\left[\frac{\eta\beta\gamma\rho\tau\,(1-v)}{\mu\,(\gamma+\mu)\,(\delta+d+\mu)}-1\right]. \tag{13}$$

Substituting this into the system's third and fourth equations, one obtains

$$E=\frac{\mu\,(\delta+d+\mu)}{\gamma\,(\alpha\mu+\beta\rho\tau)}\left[\frac{\eta\beta\gamma\rho\tau\,(1-v)}{\mu\,(\gamma+\mu)\,(\delta+d+\mu)}-1\right]. \tag{14}$$

and

$$R=\frac{\delta}{\alpha\mu+\beta\rho\tau}\left[\frac{\eta\beta\gamma\rho\tau\,(1-v)}{\mu\,(\gamma+\mu)\,(\delta+d+\mu)}-1\right]. \tag{15}$$

Finally, substituting (13) into (11) gives

$$\begin{aligned}S&=\frac{(\gamma+\mu)\,(\delta+d+\mu)\,(1+\alpha I)}{\beta\gamma\rho\tau}\\ &=\frac{(\gamma+\mu)\,(\delta+d+\mu)}{\beta\gamma\rho\tau}\,[1\\ &\quad+\frac{\mu\alpha}{\alpha\mu+\beta\rho\tau}\left[\frac{\eta\beta\gamma\rho\tau\,(1-v)}{\mu\,(\gamma+\mu)\,(\delta+d+\mu)}-1\right]\Bigg]\\ &=\frac{(\gamma+\mu)\,(\delta+d+\mu)}{\beta\gamma\rho\tau}\left[\frac{\beta\rho\tau}{\alpha\mu+\beta\rho\tau}\right.\\ &\quad\left.+\frac{\eta\beta\alpha\gamma\rho\tau\,(1-v)}{[\beta\rho\,(1-\sigma)+\mu\alpha]\,(\gamma+\mu)\,(\delta+d+\mu)}\right]\\ &=\frac{(\gamma+\mu)\,(\delta+d+\mu)}{\gamma\,(\alpha\mu+\beta\rho\tau)}\left[1+\frac{\eta\alpha\gamma\,(1-v)}{(\gamma+\mu)\,(\delta+d+\mu)}\right]\\ &=\frac{(\gamma+\mu)\,(\delta+d+\mu)+\eta\alpha\gamma\,(1-v)}{\gamma\,(\alpha\mu+\beta\rho\tau)}.\end{aligned} \tag{16}$$

This proves that

$$\mathcal{E}_1=(S_1,E_1,I_1,R_1), \tag{17}$$

where S_1, E_1, I_1, and R_1 are as given by (16), (14), (13), and (15), respectively, is the model's endemic equilibrium.

Let us now derive our model's basic reproduction number, using van den Driessche and Watmough's next-generation approach [24], [48]. First, we extract from our model (1) the equations governing the rates of change of the numbers of individuals in our infectious compartments E and I:

$$\begin{aligned}\frac{\mathrm{d}E}{\mathrm{d}t}&=F_1(S,E,I,R)-V_1(S,E,I,R),\\ \frac{\mathrm{d}I}{\mathrm{d}t}&=F_2(S,E,I,R)-V_2(S,E,I,R),\end{aligned}$$

where

$$\begin{aligned}F_1(S,E,I,R)&=\rho\tau\frac{\beta SI}{1+\alpha I},\\ F_2(S,E,I,R)&=0,\\ V_1(S,E,I,R)&=(\gamma+\mu)\,E,\\ V_2(S,E,I,R)&=-\gamma E+(\delta+d+\mu)\,I.\end{aligned}$$

Next, we evaluate the matrices

$$\mathbf{F}(S,E,I,R) = \begin{bmatrix} \dfrac{\mathrm{d}F_1(S,E,I,R)}{\mathrm{d}E} & \dfrac{\mathrm{d}F_1(S,E,I,R)}{\mathrm{d}I} \\ \dfrac{\mathrm{d}F_2(S,E,I,R)}{\mathrm{d}E} & \dfrac{\mathrm{d}F_2(S,E,I,R)}{\mathrm{d}I} \end{bmatrix} = \begin{bmatrix} 0 & \rho\tau\dfrac{\beta S}{(1+\alpha I)^2} \\ 0 & 0 \end{bmatrix}$$

and

$$\mathbf{V}(S,E,I,R) = \begin{bmatrix} \dfrac{\mathrm{d}V_1(S,E,I,R)}{\mathrm{d}E} & \dfrac{\mathrm{d}V_1(S,E,I,R)}{\mathrm{d}I} \\ \dfrac{\mathrm{d}V_2(S,E,I,R)}{\mathrm{d}E} & \dfrac{\mathrm{d}V_2(S,E,I,R)}{\mathrm{d}I} \end{bmatrix} = \begin{bmatrix} \gamma+\mu & 0 \\ -\gamma & \delta+d+\mu \end{bmatrix}$$

at the disease-free equilibrium $\mathcal{E}_0$, obtaining

$$\mathbf{F}(\mathcal{E}_0) = \begin{bmatrix} 0 & \rho\tau\dfrac{\beta(1-v)\eta}{\mu} \\ 0 & 0 \end{bmatrix}$$

and

$$\mathbf{V}(\mathcal{E}_0) = \begin{bmatrix} \gamma+\mu & 0 \\ -\gamma & \delta+d+\mu \end{bmatrix}.$$

The next-generation matrix $\mathbf{F}(\mathcal{E}_0)\left[\mathbf{V}(\mathcal{E}_0)\right]^{-1}$ of our model (1) is thus

$$\begin{bmatrix} \dfrac{\beta\eta\gamma\rho\tau(1-v)}{\mu(\gamma+\mu)(\delta+d+\mu)} & \dfrac{\beta\eta\rho\tau(1-v)}{\mu(\delta+d+\mu)} \\ 0 & 0 \end{bmatrix}. \tag{18}$$

The desired basic reproduction number is the spectral radius of the above matrix, namely,

$$\mathcal{R}_0 = \frac{\beta\eta\gamma\rho\tau(1-v)}{\mu(\gamma+\mu)(\delta+d+\mu)}.$$

It is worth mentioning that $\mathcal{R}_0$ is independent of the incidence inhibition coefficient α. Rewriting the coordinates (14), (13), and (15) of our model's endemic equilibrium (17) in terms of $\mathcal{R}_0$ and summarising our findings in this subsection, we obtain the following theorem.

Theorem 2. The model (1) has the basic reproduction number

$$\mathcal{R}_0 = \frac{\beta\eta\gamma\rho\tau(1-v)}{\mu(\gamma+\mu)(\delta+d+\mu)} \tag{19}$$

and two equilibria: the disease-free equilibrium

$$\mathcal{E}_0 = (S_0,E_0,I_0,R_0) = \left(\frac{(1-v)\eta}{\mu},0,0,0\right) \tag{20}$$

which exists for all sets of parameter values, and the endemic equilibrium

$$\mathcal{E}_1 = (S_1,E_1,I_1,R_1), \tag{21}$$

where

$$\begin{aligned} S_1 &= \frac{(\gamma+\mu)(\delta+d+\mu)+\eta\alpha\gamma(1-v)}{\gamma(\alpha\mu+\beta\rho\tau)}, \\ E_1 &= \frac{\mu(\delta+d+\mu)(\mathcal{R}_0-1)}{\gamma(\alpha\mu+\beta\rho\tau)}, \\ I_1 &= \frac{\mu(\mathcal{R}_0-1)}{\alpha\mu+\beta\rho\tau}, \\ R_1 &= \frac{\delta(\mathcal{R}_0-1)}{\alpha\mu+\beta\rho\tau}, \end{aligned}$$

which exists if and only if $\mathcal{R}_0 \geqslant 1$.

D. Stability of equilibria

Let us now study the stability of the equilibria of our model (1). For this purpose, letting

$$\begin{aligned} f_1(S,E,I,R) &= (1-v)\eta - \rho\tau\frac{\beta SI}{1+\alpha I} - \mu S, \\ f_2(S,E,I,R) &= \rho\tau\frac{\beta SI}{1+\alpha I} - (\gamma+\mu)E, \\ f_3(S,E,I,R) &= \gamma E - (\delta+d+\mu)I, \\ f_4(S,E,I,R) &= \delta I - \mu R, \end{aligned}$$

we compute the Jacobian of our model (1):

$$\mathbf{J}(S,E,I,R) = \begin{bmatrix} \dfrac{\mathrm{d}f_1}{\mathrm{d}S} & \dfrac{\mathrm{d}f_1}{\mathrm{d}E} & \dfrac{\mathrm{d}f_1}{\mathrm{d}I} & \dfrac{\mathrm{d}f_1}{\mathrm{d}R} \\ \dfrac{\mathrm{d}f_2}{\mathrm{d}S} & \dfrac{\mathrm{d}f_2}{\mathrm{d}E} & \dfrac{\mathrm{d}f_2}{\mathrm{d}I} & \dfrac{\mathrm{d}f_2}{\mathrm{d}R} \\ \dfrac{\mathrm{d}f_3}{\mathrm{d}S} & \dfrac{\mathrm{d}f_3}{\mathrm{d}E} & \dfrac{\mathrm{d}f_3}{\mathrm{d}I} & \dfrac{\mathrm{d}f_3}{\mathrm{d}R} \\ \dfrac{\mathrm{d}f_4}{\mathrm{d}S} & \dfrac{\mathrm{d}f_4}{\mathrm{d}E} & \dfrac{\mathrm{d}f_4}{\mathrm{d}I} & \dfrac{\mathrm{d}f_4}{\mathrm{d}R} \end{bmatrix} = \begin{bmatrix} -\rho\tau\dfrac{\beta I}{1+\alpha I}-\mu & 0 & -\rho\tau\dfrac{\beta S}{(1+\alpha I)^2} & 0 \\ \rho\tau\dfrac{\beta I}{1+\alpha I} & -(\gamma+\mu) & \rho\tau\dfrac{\beta S}{(1+\alpha I)^2} & 0 \\ 0 & \gamma & -(\delta+d+\mu) & 0 \\ 0 & 0 & \delta & -\mu \end{bmatrix}.$$

Evaluating this matrix at the model's disease-free equilibrium $\mathcal{E}_0$ gives the matrix $\mathbf{J}(\mathcal{E}_0)$, whose characteristic polynomial $|r\mathbf{I}-\mathbf{J}(\mathcal{E}_0)|$ is given by

$$\begin{vmatrix} r+\mu & 0 & \dfrac{\beta\eta\rho\tau(1-v)}{\mu} & 0 \\ 0 & r+\gamma+\mu & -\dfrac{\beta\eta\rho\tau(1-v)}{\mu} & 0 \\ 0 & -\gamma & r+\delta+d+\mu & 0 \\ 0 & 0 & -\delta & r+\mu \end{vmatrix}.$$

Expanding along the first and last columns gives

$$|r\mathbf{I}-\mathbf{J}(\mathcal{E}_0)| = (r+\mu)^2\left(r^2+\mathcal{A}_1 r+\mathcal{A}_2\right),$$

where

$$\begin{aligned} \mathcal{A}_1 &= \gamma+\delta+d+2\mu, \\ \mathcal{A}_2 &= \mu(\gamma+\mu)(\delta+d+\mu) - \beta\eta\gamma\rho\tau(1-v). \end{aligned}$$

Thus, of the four eigenvalues of the matrix $\mathbf{J}(\mathcal{E}_0)$, two are $-\mu$, while the remaining two are the roots of the polynomial $r^2+\mathcal{A}_1 r+\mathcal{A}_2$. Since $\mathcal{A}_1>0$, while $\mathcal{A}_2>0$ is equivalent to $\mathcal{R}_0<1$, then the Routh-Hurwitz criterion [4, sec. 4.5] implies that the disease-free equilibrium $\mathcal{E}_0$ is locally asymptotically stable if $\mathcal{R}_0<1$. If $\mathcal{R}_0=1$, then a zero eigenvalue exists, so that the disease-free equilibrium $\mathcal{E}_0$ is non-hyperbolic. If $\mathcal{R}_0>1$, then $\mathcal{A}_2<0$, and so the polynomial $r^2+\mathcal{A}_1 r+\mathcal{A}_2$, which clearly takes a positive value for a sufficiently large value of r, takes a negative value at $r=0$. By the intermediate value theorem, this ensures the existence of a positive eigenvalue, implying that the disease-free equilibrium $\mathcal{E}_0$ is unstable.

Theorem 3. The disease-free equilibrium $\mathcal{E}_0$ of the model (1) is locally asymptotically stable if $\mathcal{R}_0 < 1$, is non-hyperbolic if $\mathcal{R}_0 = 1$, and is unstable if $\mathcal{R}_0 > 1$.

On the other hand, evaluating the matrix $\mathbf{J}(S, E, I, R)$ at our model's endemic equilibrium $\mathcal{E}_1$ gives the matrix $\mathbf{J}(\mathcal{E}_1)$, whose characteristic polynomial $|r\mathbf{I} - \mathbf{J}(\mathcal{E}_1)|$ is given by

$$\begin{vmatrix} r + \dfrac{\mu\mathcal{R}_0(\alpha\mu+\beta\rho\tau)}{\mathcal{R}_0\alpha\mu+\beta\rho\tau} & 0 & \dfrac{\beta\rho\tau(\alpha\mu+\beta\rho\tau)^2 S_1}{(\mathcal{R}_0\alpha\mu+\beta\rho\tau)^2} & 0 \\ -\dfrac{\beta\rho\tau\mu(\mathcal{R}_0-1)}{\mathcal{R}_0\alpha\mu+\beta\rho\tau} & r+\gamma+\mu & -\dfrac{\beta\rho\tau(\alpha\mu+\beta\rho\tau)^2 S_1}{(\mathcal{R}_0\alpha\mu+\beta\rho\tau)^2} & 0 \\ 0 & -\gamma & r+\delta+d+\mu & 0 \\ 0 & 0 & -\delta & r+\mu \end{vmatrix}.$$

Expanding along the last column and applying an elementary row operation, one obtains that $|r\mathbf{I} - \mathbf{J}(\mathcal{E}_1)|$ can be expressed as $(r+\mu)\mathcal{D}(r)$, which implies that $-\mu$ is an eigenvalue of the matrix $\mathbf{J}(\mathcal{E}_1)$, where

$$\begin{aligned}
\mathcal{D}(r) &= \begin{vmatrix} r+\dfrac{\mu\mathcal{R}_0(\alpha\mu+\beta\rho\tau)}{\mathcal{R}_0\alpha\mu+\beta\rho\tau} & 0 & \dfrac{\beta\rho\tau(\alpha\mu+\beta\rho\tau)^2 S_1}{(\mathcal{R}_0\alpha\mu+\beta\rho\tau)^2} \\ -\dfrac{\beta\rho\tau\mu(\mathcal{R}_0-1)}{\mathcal{R}_0\alpha\mu+\beta\rho\tau} & r+\gamma+\mu & -\dfrac{\beta\rho\tau(\alpha\mu+\beta\rho\tau)^2 S_1}{(\mathcal{R}_0\alpha\mu+\beta\rho\tau)^2} \\ 0 & -\gamma & r+\delta+d+\mu \end{vmatrix} \\
&= \begin{vmatrix} r+\dfrac{\mu\mathcal{R}_0(\alpha\mu+\beta\rho\tau)}{\mathcal{R}_0\alpha\mu+\beta\rho\tau} & 0 & \dfrac{\beta\rho\tau(\alpha\mu+\beta\rho\tau)^2 S_1}{(\mathcal{R}_0\alpha\mu+\beta\rho\tau)^2} \\ r+\mu & r+\gamma+\mu & 0 \\ 0 & -\gamma & r+\delta+d+\mu \end{vmatrix} \\
&= (r+\gamma+\mu)(r+\delta+d+\mu)\left[r+\frac{\mu\mathcal{R}_0(\alpha\mu+\beta\rho\tau)}{\mathcal{R}_0\alpha\mu+\beta\rho\tau}\right] \\
&\quad - \frac{\beta\gamma\rho\tau(\alpha\mu+\beta\rho\tau)^2 S_1}{(\mathcal{R}_0\alpha\mu+\beta\rho\tau)^2}(r+\mu) \\
&= r^3 + \mathcal{B}_1 r^2 + \mathcal{B}_2 r + \mathcal{B}_3,
\end{aligned}$$

with

$$\mathcal{B}_1 = \delta + d + 2\mu + \gamma + \frac{\mu\mathcal{R}_0(\alpha\mu+\beta\rho\tau)}{\mathcal{R}_0\alpha\mu+\beta\rho\tau}, \tag{22}$$

$$\begin{aligned}
\mathcal{B}_2 &= (\gamma+\mu)(\delta+d+\mu) + (\delta+d+2\mu+\gamma)\frac{\mu\mathcal{R}_0(\alpha\mu+\beta\rho\tau)}{\mathcal{R}_0\alpha\mu+\beta\rho\tau} \\
&\quad - \frac{\beta\gamma\rho\tau(\alpha\mu+\beta\rho\tau)^2 S_1}{(\mathcal{R}_0\alpha\mu+\beta\rho\tau)^2},
\end{aligned} \tag{23}$$

$$\begin{aligned}
\mathcal{B}_3 &= (\gamma+\mu)(\delta+d+\mu)\frac{\mu\mathcal{R}_0(\alpha\mu+\beta\rho\tau)}{\mathcal{R}_0\alpha\mu+\beta\rho\tau} \\
&\quad - \frac{\mu\beta\gamma\rho\tau(\alpha\mu+\beta\rho\tau)^2 S_1}{(\mathcal{R}_0\alpha\mu+\beta\rho\tau)^2}.
\end{aligned} \tag{24}$$

Multiplying both sides of (24) by

$$\frac{(\mathcal{R}_0\alpha\mu+\beta\rho\tau)^2}{[\mu(\alpha\mu+\beta\rho\tau)]}$$

and using the expressions (16) and (19) for S_1 and $\mathcal{R}_0$, respectively, one finds that

$$\begin{aligned}
&\frac{(\mathcal{R}_0\alpha\mu+\beta\rho\tau)^2}{\mu(\alpha\mu+\beta\rho\tau)}\mathcal{B}_3 \\
&= (\gamma+\mu)(\delta+d+\mu)(\mathcal{R}_0\alpha\mu+\beta\rho\tau)\mathcal{R}_0 \\
&\quad - \beta\gamma\rho\tau(\alpha\mu+\beta\rho\tau)S_1 \\
&= (\gamma+\mu)(\delta+d+\mu)(\mathcal{R}_0\alpha\mu+\beta\rho\tau)\mathcal{R}_0 \\
&\quad - \beta\rho\tau(\gamma+\mu)(\delta+d+\mu) - \mathcal{R}_0\alpha\mu(\gamma+\mu)(\delta+d+\mu) \\
&= (\gamma+\mu)(\delta+d+\mu)(\mathcal{R}_0\alpha\mu+\beta\rho\tau)(\mathcal{R}_0-1),
\end{aligned}$$

and so

$$\mathcal{B}_3 = \frac{\mu(\gamma+\mu)(\delta+d+\mu)(\alpha\mu+\beta\rho\tau)(\mathcal{R}_0-1)}{\mathcal{R}_0\alpha\mu+\beta\rho\tau}. \tag{25}$$

Next, eliminating the terms containing S_1 in (24) and (23), one obtains that

$$\begin{aligned}
\mathcal{B}_2 &= \frac{\mathcal{B}_3}{\mu} - (\gamma+\mu)(\delta+d+\mu)\frac{\beta\rho\tau(\mathcal{R}_0-1)}{\mathcal{R}_0\alpha\mu+\beta\rho\tau} \\
&\quad + (\delta+d+2\mu+\gamma)\frac{\mu\mathcal{R}_0(\alpha\mu+\beta\rho\tau)}{\mathcal{R}_0\alpha\mu+\beta\rho\tau}.
\end{aligned} \tag{26}$$

Substituting (25) into (26) gives, after simplification,

$$\begin{aligned}
\mathcal{B}_2 &= \frac{1}{\mathcal{R}_0\alpha\mu+\beta\rho\tau}\big[(\gamma+\mu)(\delta+d+\mu)\alpha\mu(\mathcal{R}_0-1) \\
&\quad + (\delta+d+2\mu+\gamma)\mu\mathcal{R}_0(\alpha\mu+\beta\rho\tau)\big].
\end{aligned} \tag{27}$$

Therefore, if $\mathcal{R}_0 > 1$, then (22) and (25) imply that $\mathcal{B}_1 > 0$ and $\mathcal{B}_3 > 0$, while (22) and (27) imply that

$$\begin{aligned}
\mathcal{C}_1 &:= \mathcal{B}_1 - (\gamma+\mu) > 0, \\
\mathcal{C}_2 &:= \mathcal{B}_2 - (\delta+d+\mu)\frac{\mu\mathcal{R}_0(\alpha\mu+\beta\rho\tau)}{\mathcal{R}_0\alpha\mu+\beta\rho\tau} > 0,
\end{aligned}$$

and so

$$\begin{aligned}
\mathcal{B}_1\mathcal{B}_2 &= [\mathcal{C}_1 + (\gamma+\mu)]\left[\mathcal{C}_2 + (\delta+d+\mu)\frac{\mu\mathcal{R}_0(\alpha\mu+\beta\rho\tau)}{\mathcal{R}_0\alpha\mu+\beta\rho\tau}\right] \\
&> (\gamma+\mu)(\delta+d+\mu)\frac{\mu\mathcal{R}_0(\alpha\mu+\beta\rho\tau)}{\mathcal{R}_0\alpha\mu+\beta\rho\tau} \\
&> \mathcal{B}_3,
\end{aligned}$$

by (24). By the Routh-Hurwitz criterion [4, sec. 4.5], we conclude that the endemic equilibrium $\mathcal{E}_1$ is locally asymptotically stable if $\mathcal{R}_0 > 1$. If $\mathcal{R}_0 = 1$, then a zero eigenvalue exists, so that the endemic equilibrium $\mathcal{E}_1$ is non-hyperbolic. If $\mathcal{R}_0 < 1$, then, as before, the intermediate value theorem applied to the polynomial $r^3+\mathcal{B}_1 r^2+\mathcal{B}_2 r+\mathcal{B}_3$ guarantees the existence of a positive eigenvalue, implying that the endemic equilibrium $\mathcal{E}_1$ is unstable.

Theorem 4. The endemic equilibrium $\mathcal{E}_1$ of the model (1) is locally asymptotically stable if $\mathcal{R}_0 > 1$, is non-hyperbolic if $\mathcal{R}_0 = 1$, and is unstable if $\mathcal{R}_0 < 1$.

III. Discretisation

The fact that the solution of our model (1) is difficult if not impossible to obtain analytically forces us to switch our approach from analytical to numerical. To prepare a setting for our numerical simulations, in this section we discretise our model (1) using the forward Euler method [39, sec. 22.3] and study the resulting model as a discrete-time dynamical system. Specifically, we observe that the discretised

model has the same set of equilibria as our original model (subsection III-A) and derive sufficient conditions for the equilibria's local asymptotic stability which involves not only the basic reproduction number but also the discretisation step size (subsection III-B).

A. Forward Euler discretisation

We discretise the model (1) using the forward Euler method with step size $\Delta t > 0$. For every $n \geqslant 0$, we define

$$t_n = n\Delta t$$

and the approximations $\overline{S}_n \approx S(t_n)$, $\overline{E}_n \approx E(t_n)$, $\overline{I}_n \approx I(t_n)$, and $\overline{R}_n \approx R(t_n)$ generated via the recursion

$$\begin{cases} \overline{S}_{n+1} = \overline{S}_n + \left[(1-v)\,\eta - \rho\tau \dfrac{\beta \overline{S}_n \overline{I}_n}{1+\alpha \overline{I}_n} - \mu \overline{S}_n\right] \Delta t, \\ \overline{E}_{n+1} = \overline{E}_n + \left[\rho\tau \dfrac{\beta \overline{S}_n \overline{I}_n}{1+\alpha \overline{I}_n} - (\gamma+\mu)\,\overline{E}_n\right] \Delta t, \\ \overline{I}_{n+1} = \overline{I}_n + \left[\gamma \overline{E}_n - (\delta+d+\mu)\,\overline{I}_n\right] \Delta t, \\ \overline{R}_{n+1} = \overline{R}_n + \left(\delta \overline{I}_n - \mu \overline{R}_n\right) \Delta t. \end{cases} \tag{28}$$

Letting

$$\begin{aligned} \overline{f}_1\left(\overline{S},\overline{E},\overline{I},\overline{R}\right) &= \overline{S} + \left[(1-v)\eta - \rho\tau \frac{\beta \overline{S}\,\overline{I}}{1+\alpha\overline{I}} - \mu\overline{S}\right] \Delta t, \\ \overline{f}_2\left(\overline{S},\overline{E},\overline{I},\overline{R}\right) &= \overline{E} + \left[\rho\tau \frac{\beta \overline{S}\,\overline{I}}{1+\alpha\overline{I}} - (\gamma+\mu)\,\overline{E}\right] \Delta t, \\ \overline{f}_3\left(\overline{S},\overline{E},\overline{I},\overline{R}\right) &= \overline{I} + \left[\gamma\overline{E} - (\delta+d+\mu)\,\overline{I}\right] \Delta t, \\ \overline{f}_4\left(\overline{S},\overline{E},\overline{I},\overline{R}\right) &= \overline{R} + \left(\delta\overline{I} - \mu\overline{R}\right) \Delta t, \end{aligned}$$

one observes that the system of equations satisfied by the equilibria of the discrete model (28), namely,

$$\begin{cases} \overline{f}_1\left(\overline{S},\overline{E},\overline{I},\overline{R}\right) = \overline{S}, \\ \overline{f}_2\left(\overline{S},\overline{E},\overline{I},\overline{R}\right) = \overline{E}, \\ \overline{f}_3\left(\overline{S},\overline{E},\overline{I},\overline{R}\right) = \overline{I}, \\ \overline{f}_4\left(\overline{S},\overline{E},\overline{I},\overline{R}\right) = \overline{R}, \end{cases}$$

is precisely the system (9) satisfied by the equilibria of the original model (1). It follows that the discrete model (28) and the original model (1) have the same equilibria, namely, $\mathcal{E}_0$ and $\mathcal{E}_1$, as given by (20) and (21).

B. Stability of equilibria

Let us now study the stability of $\mathcal{E}_0$ and $\mathcal{E}_1$ as the equilibria of the discrete model (28). The model's Jacobian is given by

$$\overline{\mathbf{J}}\left(\overline{S},\overline{E},\overline{I},\overline{R}\right) = \begin{bmatrix} \dfrac{\mathrm{d}\overline{f}_1}{\mathrm{d}\overline{S}} & \dfrac{\mathrm{d}\overline{f}_1}{\mathrm{d}\overline{E}} & \dfrac{\mathrm{d}\overline{f}_1}{\mathrm{d}\overline{I}} & \dfrac{\mathrm{d}\overline{f}_1}{\mathrm{d}\overline{R}} \\ \dfrac{\mathrm{d}\overline{f}_2}{\mathrm{d}\overline{S}} & \dfrac{\mathrm{d}\overline{f}_2}{\mathrm{d}\overline{E}} & \dfrac{\mathrm{d}\overline{f}_2}{\mathrm{d}\overline{I}} & \dfrac{\mathrm{d}\overline{f}_2}{\mathrm{d}\overline{R}} \\ \dfrac{\mathrm{d}\overline{f}_3}{\mathrm{d}\overline{S}} & \dfrac{\mathrm{d}\overline{f}_3}{\mathrm{d}\overline{E}} & \dfrac{\mathrm{d}\overline{f}_3}{\mathrm{d}\overline{I}} & \dfrac{\mathrm{d}\overline{f}_3}{\mathrm{d}\overline{R}} \\ \dfrac{\mathrm{d}\overline{f}_4}{\mathrm{d}\overline{S}} & \dfrac{\mathrm{d}\overline{f}_4}{\mathrm{d}\overline{E}} & \dfrac{\mathrm{d}\overline{f}_4}{\mathrm{d}\overline{I}} & \dfrac{\mathrm{d}\overline{f}_4}{\mathrm{d}\overline{R}} \end{bmatrix}$$

$$= \begin{bmatrix} 1-\left(\rho\tau \dfrac{\beta\overline{I}}{1+\alpha\overline{I}} + \mu\right)\Delta t & 0 & -\rho\tau \dfrac{\beta\overline{S}}{\left(1+\alpha\overline{I}\right)^2}\Delta t & 0 \\ \rho\tau \dfrac{\beta\overline{I}}{1+\alpha\overline{I}}\Delta t & 1-(\gamma+\mu)\Delta t & \rho\tau \dfrac{\beta\overline{S}}{\left(1+\alpha\overline{I}\right)^2}\Delta t & 0 \\ 0 & \gamma\Delta t & 1-(\delta+d+\mu)\Delta t & 0 \\ 0 & 0 & \delta\Delta t & 1-\mu\Delta t \end{bmatrix}.$$

The characteristic polynomial $\left|r\mathbf{I} - \overline{\mathbf{J}}\left(\mathcal{E}_0\right)\right|$ of the matrix $\overline{\mathbf{J}}\left(\mathcal{E}_0\right)$ is given by $\left[r-(1-\mu\Delta t)\right]^2 \overline{\mathcal{D}}(r)$, where

$$\begin{aligned} \overline{\mathcal{D}}(r) &= \begin{vmatrix} r - \left[1 - (\gamma+\mu)\,\Delta t\right] & -\dfrac{\beta\eta\rho\tau\,(1-v)}{\mu}\Delta t \\ -\gamma\Delta t & r - \left[1-(\delta+d+\mu)\,\Delta t\right] \end{vmatrix} \\ &= r^2 + \overline{\mathcal{A}}_1 r + \overline{\mathcal{A}}_2, \end{aligned}$$

with

$$\begin{aligned} \overline{\mathcal{A}}_1 &= (\delta+d+2\mu+\gamma)\,\Delta t - 2, \\ \overline{\mathcal{A}}_2 &= 1 - (\delta+d+2\mu+\gamma)\,\Delta t \\ &\quad + (\gamma+\mu)\,(\delta+d+\mu)\,(1-\mathcal{R}_0)\,(\Delta t)^2. \end{aligned}$$

Now, suppose that $\mathcal{R}_0 < 1$. Let us formulate a sufficient condition for the stability of the disease-free equilibrium $\mathcal{E}_0$ of the discrete model (28). First, we require that $|1-\mu\Delta t| < 1$, which is equivalent to $\Delta t < 2/\mu$. Next, the Schur-Cohn criterion [4, sec. 2.9] for the polynomial $r^2 + \overline{\mathcal{A}}_1 r + \overline{\mathcal{A}}_2$, which reads

$$\left|\overline{\mathcal{A}}_1\right| < 1 + \overline{\mathcal{A}}_2 < 2,$$

is equivalent to

$$\Delta t < \frac{\delta+d+2\mu+\gamma}{(\gamma+\mu)\,(\delta+d+\mu)\,(1-\mathcal{R}_0)} \tag{29}$$

and

$$\left[\Delta t - \frac{\delta+d+2\mu+\gamma}{(\gamma+\mu)(\delta+d+\mu)(1-\mathcal{R}_0)}\right]^2 > \frac{\overline{\mathcal{K}}}{(\gamma+\mu)^2(\delta+d+\mu)^2(1-\mathcal{R}_0)^2},$$

where

$$\overline{\mathcal{K}} = (\delta+d+2\mu+\gamma)^2 - 4\,(\gamma+\mu)\,(\delta+d+\mu)\,(1-\mathcal{R}_0).$$

In the case $\overline{\mathcal{K}} < 0$, the latter trivially holds. In the opposite case, the latter and (29) together imply that

$$\Delta t < \frac{\delta+d+2\mu+\gamma-\sqrt{\overline{\mathcal{K}}}}{(\gamma+\mu)\,(\delta+d+\mu)\,(1-\mathcal{R}_0)}.$$

Our conclusion is the following theorem.

Theorem 5. Suppose that $\mathcal{R}_0 < 1$. The disease-free equilibrium $\mathcal{E}_0$ of the discrete model (1) is locally asymptotically stable if

$$\Delta t < \min\left\{\frac{2}{\mu}, \frac{\delta+d+2\mu+\gamma-\sqrt{\max\left\{\overline{\mathcal{K}},0\right\}}}{(\gamma+\mu)\,(\delta+d+\mu)\,(1-\mathcal{R}_0)}\right\},$$

where

$$\overline{\mathcal{K}} = (\delta+d+2\mu+\gamma)^2 - 4\,(\gamma+\mu)\,(\delta+d+\mu)\,(1-\mathcal{R}_0).$$

On the other hand, one verifies that the characteristic polynomial of the matrix $\overline{\mathbf{J}}\left(\mathcal{E}_1\right)$ is given by

$$\left|r\mathbf{I} - \overline{\mathbf{J}}\left(\mathcal{E}_1\right)\right| = \left[r-(1-\mu\Delta t)\right]\left(r^3 + \overline{\mathcal{B}}_1 r^2 + \overline{\mathcal{B}}_2 r + \overline{\mathcal{B}}_3\right),$$

where

$$\overline{\mathcal{B}}_1 = -3 + \mathcal{B}_1\Delta t,$$
$$\overline{\mathcal{B}}_2 = 3 - 2\mathcal{B}_1\Delta t + \mathcal{B}_2\left(\Delta t\right)^2,$$
$$\overline{\mathcal{B}}_3 = -1 + \mathcal{B}_1\Delta t - \mathcal{B}_2\left(\Delta t\right)^2 + \mathcal{B}_3\left(\Delta t\right)^3,$$

with $\mathcal{B}_1$, $\mathcal{B}_2$, and $\mathcal{B}_3$ as defined by (22), (23), and (24). In the case $\mathcal{R}_0 > 1$, we have that

$$1 + \overline{\mathcal{B}}_1 + \overline{\mathcal{B}}_2 + \overline{\mathcal{B}}_3 = \mathcal{B}_3\left(\Delta t\right)^3 > 0$$

by (25), so that the Schur-Cohn criterion [4, sec. 2.9] for the polynomial $r^3 + \overline{\mathcal{B}}_1 r^2 + \overline{\mathcal{B}}_2 r + \overline{\mathcal{B}}_3$ implies the following theorem.

Theorem 6. Suppose that $\mathcal{R}_0 > 1$. The endemic equilibrium $\mathcal{E}_1$ of the discrete model (28) is locally asymptotically stable if $\Delta t < 2/\mu$ and the following three inequalities hold:

- $8 - 4\mathcal{B}_1\Delta t + 2\mathcal{B}_2\left(\Delta t\right)^2 - \mathcal{B}_3\left(\Delta t\right)^3 > 0$,
- $4\mathcal{B}_1 - 2\left(\mathcal{B}_1^2 + 2\mathcal{B}_2\right)\Delta t + \left(3\mathcal{B}_1\mathcal{B}_2 + 5\mathcal{B}_3\right)\left(\Delta t\right)^2 - \left(3\mathcal{B}_1\mathcal{B}_3 + \mathcal{B}_2^2\right)\left(\Delta t\right)^3 + 2\mathcal{B}_2\mathcal{B}_3\left(\Delta t\right)^4 - \mathcal{B}_3^2\left(\Delta t\right)^5 > 0$,
- $\mathcal{B}_1\mathcal{B}_2 - \mathcal{B}_3 - \left(\mathcal{B}_1\mathcal{B}_3 + \mathcal{B}_2^2\right)\Delta t + 2\mathcal{B}_2\mathcal{B}_3\left(\Delta t\right)^2 - \mathcal{B}_3^2\left(\Delta t\right)^3 > 0$,

where $\mathcal{B}_1$, $\mathcal{B}_2$, and $\mathcal{B}_3$ are as defined by (22), (23), and (24), respectively.

IV. Numerical simulations and sensitivity analysis

Let us now employ our discretised model (28) to generate numerical solutions of our original model (1), using the parameter values provided in Table I. Many of these parameter values are derived from the work of Al-Harbi and Al-Tuwairqi [3]. These authors, firstly, estimated the birth rate η and the natural death coefficient μ using the average life span in Saudi Arabia: 75 years [3, Tbl. 1]. In addition, they estimated the incubation coefficient γ using the median incubation period of COVID-19 in Saudi Arabia: 6 days [3, Tbl. 1]. Subsequently, employing the data of the active cases of COVID-19 from March 12, 2020 to September 23, 2020 provided by the Saudi Ministry of Health, the same authors carried out a nonlinear least-squares curve-fitting to estimate the incidence, recovery, and death-by-disease coefficients β, δ, and d [3, Tbl. 1]. The values for the other parameters: the vaccination proportion v, the lockdown intensity $1 - \rho$, the social-distancing intensity $1 - \tau$, the incidence inhibition coefficient α, and the initial number of individuals in each compartment $S(0)$, $E(0)$, $I(0)$, and $R(0)$, are all simulated. Notice that Table I specifies two different sets of parameter values, differing only on the values of the vaccination proportion v. As we shall see, the higher value $v = 0.8$ leads to a disease-free case (subsection IV-A), while the lower value $v = 0.1$ leads to an endemic case (subsection IV-B). For each case, we shall visualise the time-evolution of the number of individuals in each compartment as governed by our discretised model (28). In the disease-free case, we conduct a sensitivity analysis of the basic reproduction number with respect to each parameter, whereas in the endemic case, we conduct a sensitivity analysis of not only the basic reproduction number but also the epidemic peak —the maximum number of infectious individuals— with respect to each parameter.

A. A disease-free case

Using the parameter values in Table I with $v = 0.8$, the basic reproduction number (19) evaluates to $\mathcal{R}_0 \approx 0.3774 < 1$, and the model's disease-free equilibrium (20) reads

$$\mathcal{E}_0 \approx (6250,\, 0,\, 0,\, 0)\,.$$

By Theorem 5, this equilibrium of the discrete model (28) is stable if $\Delta t < 2.8543$. Choosing $\Delta t = 0.4$, we generate the plots visualising the time-evolution of the numbers of susceptible, exposed, infected, and recovered individuals as governed by the model (28), presented in Figure 2. Evidently, the dynamics of the number of susceptible individuals, beginning at 2999, is characterised by an initial sharp increase and a monotonic convergence towards the equilibrium value of 6250. Conversely, the dynamics of the number of exposed individuals, beginning at 1, is characterised by an initial sharp decrease and a monotonic convergence towards the equilibrium value of 0. On the other hand, the numbers of infected and recovered individuals both display non-monotonic convergence towards 0. Consequently, as expected, the population becomes disease-free at the equilibrium state.

To determine an appropriate strategy for the preservation of such disease-free condition, let us carry out a sensitivity analysis of the basic reproduction number with respect to our model's parameters. The availability of the expression (19) of the basic reproduction number as a differentiable function of the parameters presented in Table I enables us to compute analytically the sensitivity index

$$\Upsilon_p^{\mathcal{R}_0} = \frac{\partial \mathcal{R}_0}{\partial p} \cdot \frac{p}{\mathcal{R}_0}$$

of $\mathcal{R}_0$ with respect to each of our model's parameter $p \in \{v, \eta, \rho, \tau, \beta, \alpha, \mu, d, \gamma, \delta\}$ [21]. The computation yields

$$\Upsilon_v^{\mathcal{R}_0} = -\frac{v}{1-v}, \qquad \Upsilon_\eta^{\mathcal{R}_0} = \Upsilon_\rho^{\mathcal{R}_0} = \Upsilon_\tau^{\mathcal{R}_0} = \Upsilon_\beta^{\mathcal{R}_0} = 1,$$
$$\Upsilon_\alpha^{\mathcal{R}_0} = 0,$$
$$\Upsilon_\mu^{\mathcal{R}_0} = -\frac{3\mu^2 + 2\left(\delta + d + \gamma\right)\mu + \left(\delta + d\right)\gamma}{\left(\gamma + \mu\right)\left(\delta + d + \mu\right)},$$
$$\Upsilon_d^{\mathcal{R}_0} = -\frac{d}{\delta + d + \mu}, \qquad \Upsilon_\gamma^{\mathcal{R}_0} = \frac{\mu}{\gamma + \mu},$$
$$\text{and} \qquad \Upsilon_\delta^{\mathcal{R}_0} = -\frac{\delta}{\delta + d + \mu}.$$

Since our model (1) is a modification of the model by Al-Harbi and Al-Tuwairqi [3], it is not surprising that the sensitivity indices $\Upsilon_\eta^{\mathcal{R}_0}$, $\Upsilon_\rho^{\mathcal{R}_0}$, $\Upsilon_\beta^{\mathcal{R}_0}$, $\Upsilon_\mu^{\mathcal{R}_0}$, $\Upsilon_d^{\mathcal{R}_0}$, $\Upsilon_\gamma^{\mathcal{R}_0}$, and $\Upsilon_\delta^{\mathcal{R}_0}$ are the same as those computed by Al-Harbi and Al-Tuwairqi using their original model [3, p. 16]. Evaluating the above indices for the parameter values given in Table I with $v = 0.8$, we obtain the values listed in the second column of Table II. Observing that $\Upsilon_v^{\mathcal{R}_0}$ is significantly larger in absolute value compared to the other sensitivity indices including $\Upsilon_\tau^{\mathcal{R}_0}$ and $\Upsilon_\rho^{\mathcal{R}_0}$, we conclude that, as a strategy to preserve the disease-free condition, maintaining the high value of the vaccination proportion is more important than maintaining the enforcement of social distancings or lockdowns. In fact, substituting all the disease-free parameter values apart from τ and ρ into the expression (19), one obtains an expression for $\mathcal{R}_0$ as a bivariate function of τ and ρ, for which the inequality $\mathcal{R}_0\left(\tau, \rho\right) < 1$ holds for every

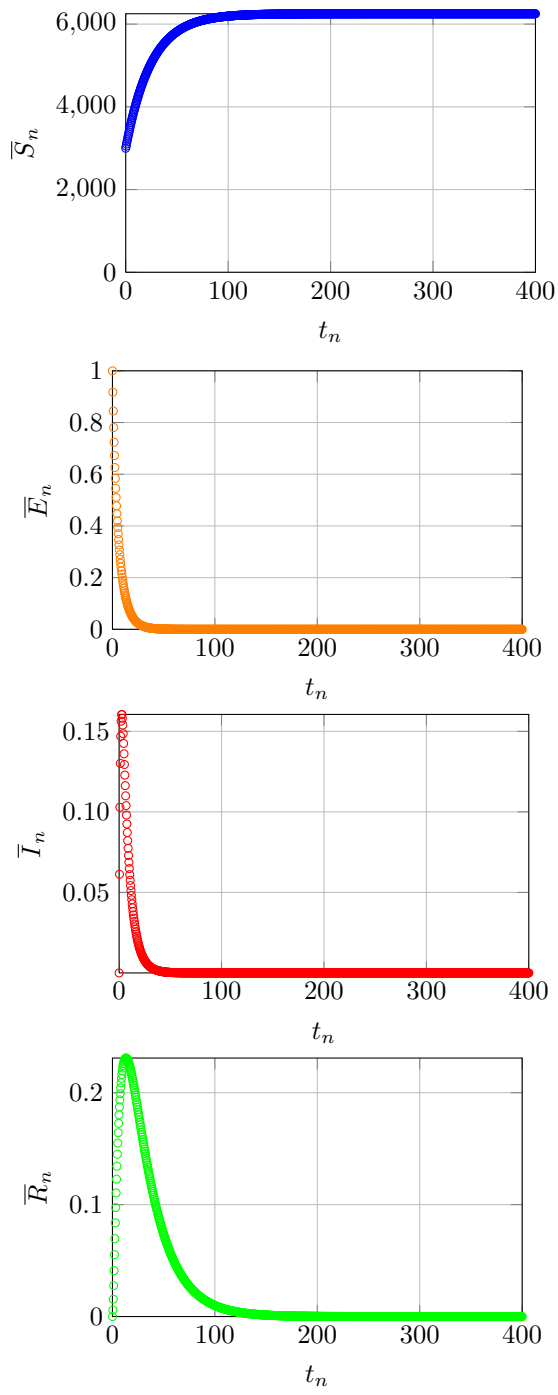

Fig. 2. Plots of $\overline{S}_n$, $\overline{E}_n$, $\overline{I}_n$, and $\overline{R}_n$ versus t_n for $n \in \{0, \ldots, 1000\}$ using parameter values listed in Table I, with $v = 0.8$ and $\Delta t = 0.4$.

$\tau \in [0, 1]$ and $\rho \in [0, 1]$. This implies that, provided the high value of the vaccination proportion $v = 0.8$ is sustained, the population will remain disease-free even if social distancing and lockdown restrictions are entirely lifted.

B. An endemic case

For an endemic case, let us employ the parameter values in Table I with the low vaccination proportion $v = 0.1$. Substituting these into the expression (19) gives $\mathcal{R}_0 \approx 1.6984 > 1$. Furthermore, the model's endemic equilibrium (21) reads

$$\mathcal{E}_1 \approx (17498,\ 2054,\ 567,\ 3362)\,.$$

TABLE II
VALUES OF THE SENSITIVITY INDICES OF THE BASIC REPRODUCTION NUMBER OF OUR MODEL FOR PARAMETER VALUES LISTED IN TABLE I, WITH v AS IN THE FIRST ROW.

Sensitivity index	$v = 0.8$, $\mathcal{R}_0 \approx 0.3774 < 1$	$v = 0.1$, $\mathcal{R}_0 \approx 1.6984 > 1$
$\Upsilon_v^{\mathcal{R}_0}$	-4.0000	-0.1111
$\Upsilon_\eta^{\mathcal{R}_0}$	1.0000	1.0000
$\Upsilon_\rho^{\mathcal{R}_0}$	1.0000	1.0000
$\Upsilon_\tau^{\mathcal{R}_0}$	1.0000	1.0000
$\Upsilon_\beta^{\mathcal{R}_0}$	1.0000	1.0000
$\Upsilon_\alpha^{\mathcal{R}_0}$	0.0000	0.0000
$\Upsilon_\mu^{\mathcal{R}_0}$	-1.2594	-1.2594
$\Upsilon_d^{\mathcal{R}_0}$	-0.3922	-0.3922
$\Upsilon_\gamma^{\mathcal{R}_0}$	0.1932	0.1932
$\Upsilon_\delta^{\mathcal{R}_0}$	-0.3922	-0.3922

The first of the sufficient conditions for the stability of this equilibrium of the discrete model (28) as prescribed by Theorem 6 reads $\Delta t < 50$, and evaluating the constants defined in (22), (23), and (24),

$$\mathcal{B}_1 \approx 0.8763, \quad \mathcal{B}_2 \approx 0.0589, \quad \text{and} \quad \mathcal{B}_3 \approx 0.0033,$$

one verifies that $\Delta t = 0.4$ satisfies the three inequalities stated in the theorem. Using the same value of Δt, we generate the time-evolution plots displayed in Figure 3. Observe that the convergence towards the endemic equilibrium occurs in a non-monotonic manner. The infectious population size, plotted against time in Figure 4, reaches a maximum of

$$\mathcal{I}_{\max} = \max\left\{\overline{E}_n + \overline{I}_n : n \in \{0, \ldots, 1000\}\right\} \approx 3725.8723$$

at time $t_{\max} = 153.2$.

Let us now turn to our sensitivity analysis of the basic reproduction number in this endemic case. Among all sensitivity indices computed in subsection IV-A, we note that only $\Upsilon_v^{\mathcal{R}_0}$ depends on v. Consequently, as apparent from the third column of Table II, the values of all sensitivity indices in this endemic case are the same as those in the disease-free case, with the exception of $\Upsilon_v^{\mathcal{R}_0}$, which evaluates to -0.1111 in this endemic case. The fact that $\left|\Upsilon_\rho^{\mathcal{R}_0}\right| = \left|\Upsilon_\tau^{\mathcal{R}_0}\right| = 1.0000 > 0.1111 = \left|\Upsilon_v^{\mathcal{R}_0}\right|$ implies that, as a strategy to suppress the value of the basic reproduction number in this endemic case, the intensification of social distancing and lockdown is more effective than the distribution of vaccines.

The fact that the infectious population size, as a function of time, possesses a unique maximum $\mathcal{I}_{\max}$, the epidemic peak, as apparent from Figure 4, motivates the determination of a strategy which is most effective to lower this peak. For this purpose, we wish to conduct a sensitivity analysis of $\mathcal{I}_{\max}$ with respect to our model's parameters. However, since an analytical expression of $\mathcal{I}_{\max}$ as a function of the parameters is not readily available, we employ the following estimate for $\Upsilon_p^{\mathcal{I}_{\max}}$:

$$\overline{\Upsilon}_p^{\mathcal{I}_{\max}}(\Psi) = \frac{1}{|\Psi|} \sum_{\psi \in \Psi} \frac{\rho_{\mathcal{I}_{\max},p}(\psi)}{\psi},$$

where $\Psi = \{-10\%, -5\%, 5\%, 10\%\}$ and $\rho_{\mathcal{I}_{\max},p}(\psi)$ is the relative change in the value of $\mathcal{I}_{\max}$ due to a change of ψ in the value of p. Our computation of $\overline{\Upsilon}_p^{\mathcal{I}_{\max}}(\Psi)$

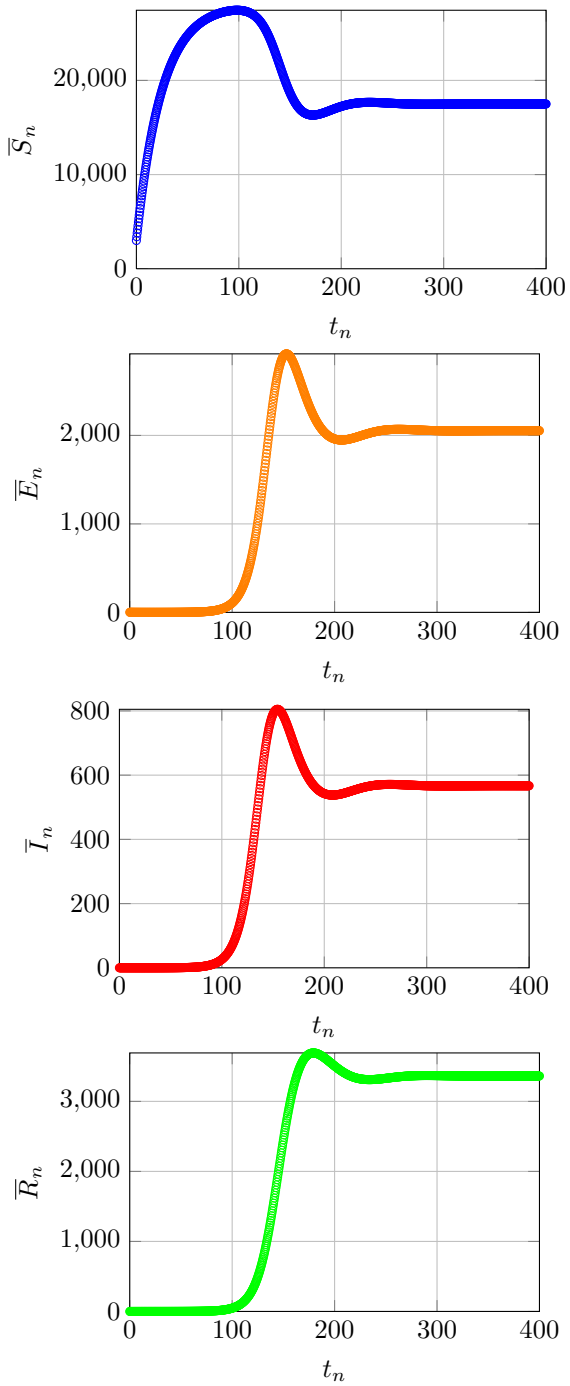

Fig. 3. Plots of $\overline{S}_n$, $\overline{E}_n$, $\overline{I}_n$, and $\overline{R}_n$ versus t_n for $n \in \{0, \ldots, 1000\}$ using parameter values listed in Table I, with $v = 0.1$ and $\Delta t = 0.4$.

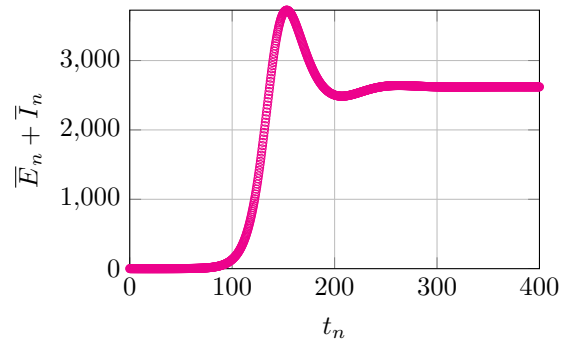

Fig. 4. Plot of $\overline{E}_n + \overline{I}_n$ versus t_n for $n \in \{0, \ldots, 1000\}$ using parameter values listed in Table I, with $v = 0.1$ and $\Delta t = 0.4$.

TABLE III
ESTIMATION OF THE SENSITIVITY INDICES OF $\mathcal{I}_{\max}$ WITH RESPECT TO OUR MODEL'S PARAMETERS, USING PARAMETER VALUES LISTED IN TABLE I, WITH $v = 0.1$ AND $\Delta t = 0.4$.

p	ψ	$\rho_{\mathcal{I}_{\max},p}(\psi)$	$\rho_{\mathcal{I}_{\max},p}(\psi)/\psi$	$\overline{\Upsilon}_p^{\mathcal{I}_{\max}}(\Psi)$
v	10%	−3.4108%	−0.3411	−0.3420
	5%	−1.7072%	−0.3414	
	−5%	1.7112%	−0.3422	
	−10%	3.4312%	−0.3431	
η	10%	31.4487%	3.1449	3.0698
	5%	15.5700%	3.1140	
	−5%	−15.1791%	3.0358	
	−10%	−29.8458%	2.9846	
ρ	10%	21.0648%	2.1065	2.2108
	5%	10.8004%	2.1601	
	−5%	−11.3231%	2.2646	
	−10%	−23.1183%	2.3118	
τ	10%	21.0648%	2.1065	2.2108
	5%	10.8004%	2.1601	
	−5%	−11.3231%	2.2646	
	−10%	−23.1183%	2.3118	
β	10%	21.0648%	2.1065	2.2108
	5%	10.8004%	2.1601	
	−5%	−11.3231%	2.2646	
	−10%	−23.1183%	2.3118	
α	10%	−1.3816%	−0.1382	−0.1403
	5%	−0.6960%	−0.1392	
	−5%	0.7067%	−0.1413	
	−10%	1.4243%	−0.1424	
μ	10%	−30.0007%	−3.0001	−3.3498
	5%	−15.8539%	−3.1708	
	−5%	17.6213%	−3.5243	
	−10%	37.0389%	−3.7039	
d	10%	−8.3960%	−0.8396	−3.3498
	5%	−4.2395%	−0.8479	
	−5%	4.3200%	−0.8640	
	−10%	8.7245%	−0.8724	
γ	10%	0.8461%	0.0846	0.1084
	5%	0.4763%	0.0953	
	−5%	−0.5977%	0.1195	
	−10%	−1.3415%	0.1342	
δ	10%	−11.5125%	−1.1512	−1.1826
	5%	−5.8349%	−1.1670	
	−5%	5.9916%	−1.1983	
	−10%	12.1367%	−1.2137	

for $p \in \{v, \eta, \rho, \tau, \beta, \alpha, \mu, d, \gamma, \delta\}$ is presented in Table III. Since $\left|\overline{\Upsilon}_\tau^{\mathcal{I}_{\max}}(\Psi)\right| \approx \left|\overline{\Upsilon}_\rho^{\mathcal{I}_{\max}}(\Psi)\right| \approx 2.2108 > 0.3420 \approx \left|\overline{\Upsilon}_v^{\mathcal{I}_{\max}}(\Psi)\right|$, we conclude that the intensification of social distancing and lockdown is significantly more effective in lowering the epidemic peak compared to the distribution of vaccines.

V. CONCLUSIONS AND FUTURE RESEARCH

We have constructed a modification of an SEIR-type disease-transmission model, originally proposed by Al-Harbi and Al-Tuwairqi to study the impact of social distancings and lockdowns on the transmission of COVID-19 in Saudi Arabia [3]. Our modified model features two additional parameters: the proportion of vaccinated newborns and the

incidence inhibition coefficient, the former allowing a comparison of three eradication strategies: social distancing, lockdown, and vaccination. We have established the non-negativity and boundedness of the model's solutions, showed that the model possesses two equilibria: disease-free and endemic, and obtained an expression for the model's basic reproduction number $\mathcal{R}_0$ as a function of the involved parameters. We have also proved that the disease-free equilibrium is locally asymptotically stable if $\mathcal{R}_0 < 1$, and that the endemic equilibrium is locally asymptotically stable if $\mathcal{R}_0 > 1$. Subsequently, we have discretised our model using the forward Euler method, and showed that the resulting discrete model possesses the same equilibria. We have also formulated conditions on the discretisation step size for the local asymptotic stability of the disease-free equilibrium in the case $\mathcal{R}_0 < 1$, and for that of the endemic equilibrium in the case $\mathcal{R}_0 > 1$. Finally, we have employed our discrete model to generate numerical solutions of our original model, and carried out a sensitivity analysis using two sets of parameter values, representing the cases $\mathcal{R}_0 < 1$ and $\mathcal{R}_0 > 1$. The results showed that, for preventing an outbreak in a disease-free situation, vaccination is more effective than social distancing and lockdown, whereas for resolving an endemic situation and lowering the epidemic peak, social distancing and lockdown are more effective than vaccination.

This research is extendible in numerous ways. First, one could attempt to establish the global asymptotic stability of the equilibria of our model and its discretisation using Lyapunov functions [48, sec. 7.3], as demonstrated by Al-Harbi and Al-Tuwairqi for their original model [3, sec. 3.3]. In addition, our model itself could be further modified to incorporate currently unconsidered parameters, such as the vaccine's efficacy [23], [28], [69], [70], the hospitals' bed-occupancy rate [19], [50], [71], or the influence of mass media [18], [43], [49], [65], and to accommodate other vaccination strategies, such as pulse vaccination [30], [44], [46], [60], [61]. One could also replace not only the Holling type II incidence rate but also the linear recovery rate with various alternative forms [52]. Finally, one could also extend our study through an actuarial viewpoint, by designing a health-and-life insurance policy based on our disease-transmission model, and conducting a financial analysis of the policy [11], [27], [32], [34], [51], [53], [72].

REFERENCES

[1] A. Abidemi, M. I. A. Aziz, and R. Ahmad, "The impact of vaccination, individual protection, treatment and vector controls on dengue," Engineering Letters, vol. 27, no. 3, pp613-622, 2019.

[2] D. Alboaneen, B. Pranggono, D. Alshammari, N. Alqahtani, and R. Alyaffer, "Predicting the epidemiological outbreak of the coronavirus disease 2019 (COVID-19) in Saudi Arabia," International Journal of Environmental Research and Public Health, vol. 17, no. 12, 4568, 2020.

[3] S. K. Al-Harbi and S. M. Al-Tuwairqi, "Modeling the effect of lockdown and social distancing on the spread of COVID-19 in Saudi Arabia," PLoS ONE, vol. 17, no. 4, e0265779, 2022.

[4] L. J. S. Allen, An Introduction to Mathematical Biology, Pearson, New Jersey, 2007.

[5] S. Alrashed, N. Min-Allah, A. Saxena, I. Ali, and R. Mehmood, "Impact of lockdowns on the spread of COVID-19 in Saudi Arabia," Informatics in Medicine Unlocked, vol. 20, 100420, 2020.

[6] F. S. Alshammari, "A mathematical model to investigate the transmission of COVID-19 in the kingdom of Saudi Arabia," Computational and Mathematical Methods in Medicine, vol. 2020, no. 1, 9136157, 2020.

[7] S. I. Alzahrani, I. A. Aljamaan, and E. A. Al-Fakih, "Forecasting the spread of the COVID-19 pandemic in Saudi Arabia using ARIMA prediction model under current public health interventions," Journal of Infection and Public Health, vol. 13, no. 7, pp914-919, 2020.

[8] R. G. Amballoor and S. B. Naik, "Dissemination of firm's market information: Application of Kermack-Mckendrick SIR model," in Advances in Computing and Data Sciences (eds. M. Singh, V. Tyagi, P. K. Gupta, J. Flusser, T. Ören, and V. R. Sonawane), Springer, (2021), pp22-32.

[9] R. G. Amballoor and S. B. Naik, "SIR model for understanding the spread of fake news and hate speech," in Text and Social Media Analytics for Fake News and Hate Speech Detection (eds. H. K. Soni, S. Sharma, and G. R. Sinha), CRC Press, (2024), pp166-180.

[10] R. Artiono, B. P. Prawoto, D. Hidayat, D. N. Yunianti, and Y. P. Astuti, "The dynamics of COVID-19: the effect of large-scale social restrictions," Communications in Mathematical Biology and Neuroscience, vol. 2020, 76, 2020.

[11] F. Atatalab, A. T. P. Najafabadi, and M. Zokaei, Designing an epidemic health insurance, preprint, Research Square, 2022.

[12] M. A. Aziz-Alaoui, F. Najm, and R. Yafia, "SIARD model and effect of lockdown on the dynamics of COVID-19 disease with non total immunity," Mathematical Modelling of Natural Phenomena, vol. 16, 31, 2021.

[13] M. Bachar, M. A. Khamsi, and M. Bounkhel, "A mathematical model for the spread of COVID-19 and control mechanisms in Saudi Arabia," Advances in Difference Equations, vol. 2021, no. 1, 253, 2021.

[14] S. Bahri, A. Mardiyah, A. I. Baqi, and A. Zakiyyah, "Local stability analysis and simulation of Omicron virus spread using the Omicron SSvIR model," IAENG Journal of Applied Mathematics, vol. 54, no. 5, pp797-803, 2024.

[15] S. K. Bhatia, S. Chauhan, and U. Nasir, "Dynamics of vaccination model with Holling type II functional response," Kyungpook Mathematical Journal, vol. 60, no. 2, pp319-334, 2020.

[16] S. Bugalia, V. P. Bajiya, J. P. Tripathi, M. T. Li, and G. Q. Sun, "Mathematical modeling of COVID-19 transmission: The roles of intervention strategies and lockdown," Mathematical Biosciences and Engineering, vol. 17, no. 5, pp5961-5986, 2020.

[17] Y. Chakir, "Global approximate solution of SIR epidemic model with constant vaccination strategy," Chaos, Solitons and Fractals, vol. 169, 113323, 2023.

[18] A. Chatterjee and S. Ganguly, "Modeling the impact of media coverage on the spread of infectious diseases: The curse of the twenty-first century," in Trends in Biomathematics: Modeling Epidemiological, Neuronal, and Social Dynamics (ed. R. P. Mondaini), Springer, (2022), pp153-169.

[19] Z. Chen and G. Kong, "Hospital admission, facilitybased isolation, and social distancing: An SEIR model with constrained medical resources," Production and Operations Management, vol. 32, no. 5, pp1397-1414, 2023.

[20] K. Chinnadurai, S. Athithan, and M. G. Fajlul Kareem, "Mathematical modelling on alcohol consumption control and its effect on poor population," IAENG International Journal of Applied Mathematics, vol. 54, no. 1, pp1-9, 2024.

[21] N. Chitnis, J. M. Hyman, and J. M. Cushing, "Determining important parameters in the spread of malaria through the sensitivity analysis of a mathematical model," Bulletin of Mathematical Biology, vol. 70, pp1272-1296, 2008.

[22] A. M. del Rey, R. C. Vara, S. R. González, "A computational propagation model for malware based on the SIR classic model," Neurocomputing, vol. 484, pp161-171, 2022.

[23] M. L. Diagne, H. Rwezaura, S. Y. Tchoumi, and J. M. Tchuenche, "A mathematical model of COVID-19 with vaccination and treatment," Computational and Mathematical Methods in Medicine, vol. 2021, no. 1, 1250129, 2021.

[24] P. van den Driessche and J. Watmough, "Reproduction numbers and sub-threshold endemic equilibria for compartmental models of disease transmission," Mathematical Biosciences, vol. 180, no. 1-2, pp29-48, 2002.

[25] S. Federico, G. Ferrari, and M. L. Torrente, "Optimal vaccination in a SIRS epidemic model," Economic Theory, vol. 77, no. 1, pp49-74, 2024.

[26] L. Fei and H. Lv, "Multi-host transmission dynamics of schistosomiasis and effective control," IAENG International Journal of Applied Mathematics, vol. 54, no. 11, pp2316-2329, 2024.

[27] R. H. Feng and J. Garrido, "Actuarial applications of epidemic models," North American Actuarial Journal, vol. 15, no. 1, pp112-136, 2011.

[28] B. H. Foy, B. Wahl, K. Mehta, A. Shet, G. I. Menon, C. Britto, "Comparing COVID-19 vaccine allocation strategies in India: A mathematical modelling study," International Journal of Infectious Diseases, vol. 103, pp431-438, 2021.

[29] Y. Fu, H. Xiang, H. Jin, and N. Wang, "Mathematical modelling of lockdown policy for COVID-19," Procedia Computer Science, vol. 187, pp447-457, 2021.

[30] E. C. Gabrick, E. L. Brugnago, S. L. T. de Souza, K. C. Iarosz, J. D. Szezech, R. L. Viana, I. L. Caldas, A. M. Batista, and J. Kurths, "Impact of periodic vaccination in SEIRS seasonal model," Chaos: An Interdisciplinary Journal of Nonlinear Science, vol. 34, no. 1, 013137 2024.

[31] S. Gounane, Y. Barkouch, A. Atlas, M. Bendahmane, F. Karami, and D. Meskine, "An adaptive social distancing SIR model for COVID-19 disease spreading and forecasting," Epidemiologic Methods, vol. 10, no. s1, 20200044, 2021.

[32] D. Hainaut, "An actuarial approach for modeling pandemic risk," Risks, vol. 9, 2021, 3.

[33] J. L. M. Hamzah, H. N. Fadhilah, and R. Syaifullah, "Analysis of the SEIR model for measles spread with the influence of vaccination," IAENG Journal of Applied Mathematics, vol. 55, no. 3, pp626-635, 2025.

[34] J. Hoseana, F. Kusnadi, G. Stephanie, L. Loanardo, and C. Wijaya, "Design and financial analysis of a health insurance based on an SIH-type epidemic model," Journal of Mathematics and Computer Science, vol. 38, no. 2, pp160-178, 2025.

[35] C. Jana, A. P. Maiti, and D. K. Maiti, "Complex dynamical behavior of a ratio-dependent eco-epidemic model with Holling type-II incidence rate in the presence of two delays," Communications in Nonlinear Science and Numerical Simulation, vol. 110, 106380, 2022.

[36] A. J. Kadhim and A. A. Majeed, "Epidemiological model involving two diseases in predator population with Holling type-II functional response," International Journal of Nonlinear Analysis and Applications, vol. 12, no. 2, pp2085-2107, 2021.

[37] L. Kalachev, E. L. Landguth, J. Graham, "Revisiting classical SIR modelling in light of the COVID-19 pandemic," Infectious Disease Modelling, vol. 8, no. 1, pp72-83, 2023.

[38] W. O. Kermack and A. G. McKendrick, "A contribution to the mathematical theory of epidemics," Proceedings of the Royal Society of London, vol. 115, no. 772, pp700-721, 1927.

[39] Q. Kong, T. Siauw, and A. Bayen, Python Programming and Numerical Methods: A Guide for Engineers and Scientists, Academic Press, London, 2021.

[40] M. Kreck and E. Scholz, "Back to the roots: A discrete KermackMcKendrick model adapted to Covid-19," Bulletin of Mathematical Biology, vol. 84, no. 4, 44, 2022.

[41] L. B. Kunwar and V. S. Verma, "Mathematical analysis of alcoholism with effect of awareness through media in developing countries," Engineering Letters, vol. 31, no. 1, pp295-304, 2023.

[42] R. Lamoonwong and E. Kunnawuttipreechachan, "Stability of the SIRS epidemic models with general transmission rate functions," IAENG International Journal of Applied Mathematics, vol. 53, no. 4, pp1492-1503, 2023.

[43] K. Lata, A. K. Misra, and Y. Takeuchi, "Modeling the effectiveness of TV and social media advertisements on the dynamics of water-borne diseases," International Journal of Biomathematics, vol. 15, no. 2, 2150069, 2022

[44] C. Li and J. Lu, "Novel corona virus disease dynamical models with pulse vaccination," Results in Physics, vol. 53, 107028, 2023.

[45] Z. Ma and J. Li, Dynamical Modeling and Analysis of Epidemics, World Scientific, Singapore, 2009.

[46] Y. Ma and X. Zuo, "Stability analysis of SIRS model considering pulse vaccination and elimination disturbance," Journal of Mathematics, vol. 2024, no. 1, 6617911, 2024.

[47] T. T. Marinov and R. S. Marinova, "Inverse problem for adaptive SIR model: Application to COVID-19 in Latin America," Infectious Disease Modelling, vol. 7, no. 1, pp134-148, 2022.

[48] M. Martcheva, An Introduction to Mathematical Epidemiology, Springer, New York, 2015.

[49] R. Medda, S. Pal, and J. Bhattacharyya, "Modelling the role of TV and internet coverage on mitigating the spread of infectious diseases," in Trends in Biomathematics: Stability and Oscillations in Environmental, Social, and Biological Models (ed. R. P. Mondaini), Springer, (2022), pp383-405.

[50] A. K. Misra and J. Maurya, "Bifurcation analysis and optimal control of an epidemic model with limited number of hospital beds," International Journal of Biomathematics, vol. 16, no. 4, 2250101, 2023.

[51] H. S. Nam, "Mathematical and actuarial analysis on a deterministic SEIR model," Global Journal of Pure and Applied Mathematics, vol. 18, no. 2, pp453-464, 2022.

[52] Nilam, "Cause and control strategy for infectious diseases with nonlinear incidence and treatment rate," in Mathematical Modelling and Analysis of Infectious Diseases (eds. K. Hattaf and H. Dutta), Springer, (2020), pp61-81.

[53] C. I. Nkeki and G. O. S. Ekhaguere, "Some actuarial mathematical models for insuring the susceptibles of a communicable disease," International Journal of Financial Engineering, vol. 7, no. 2, 2050014, 2020.

[54] S. Olaniyi, M. A. Lawal, and O. S. Obabiyi, "Stability and sensitivity analysis of a deterministic epidemiological model with pseudo-recovery," IAENG International Journal of Applied Mathematics, vol. 46, no. 2, pp160-167, 2016.

[55] R. Ramesh and G. A. Joseph, "The optimal control methods for the COVID-19 pandemic model's precise and practical SIQR mathematical model," IAENG International Journal of Applied Mathematics, vol. 54, no. 8, pp1657-1672, 2024.

[56] R. C. Robinson, An Introduction to Dynamical Systems: Continuous and Discrete, 2nd ed., American Mathematical Society, Rhode Island, 2012.

[57] S. Saha and G. P. Samanta, "Analysis of a COVID-19 model implementing social distancing as an optimal control strategy," in Integrated Science of Global Epidemics (ed. N. Rezaei), Springer, (2023), pp211-258.

[58] A. Saman, S. Side, M. I. Pratama, and W. Sanusi, "Optimal control of the SEIR model of online game addiction using guidance and counseling," Engineering Letters, vol. 30, no. 3, pp1152-1156, 2022.

[59] S. Sharma and P. K. Sharma, "A study of SIQR model with Holling type-II incidence rate," Malaya Journal of Matematik, vol. 9, no. 1, pp305-311, 2021.

[60] B. Shulgin, L. Stone, and Z. Agur, "Pulse vaccination strategy in the SIR epidemic model," Bulletin of Mathematical Biology, vol. 60, no. 6, pp1123-1148, 1998.

[61] L. Stone, B. Shulgin, and Z. Agur, "Theoretical examination of the pulse vaccination policy in the SIR epidemic model," Mathematical and Computer Modelling, vol. 31, no. 4-5, pp207-215, 2000.

[62] S. H. Strogatz, Nonlinear Dynamics and Chaos, 2nd ed., CRC Press, Boca Raton, 2018.

[63] C. Sun, W. Yang, J. Arino, and K. Khan, "Effect of media-induced social distancing on disease transmission in a two patch setting," Mathematical Biosciences, vol. 230, no. 2, pp87-95, 2011.

[64] R. Thamchai, "Optimal control of a drinking epidemic model with time delay," IAENG International Journal of Applied Mathematics, vol. 55, no. 5, pp1205-1212, 2025.

[65] P. K. Tiwari, R. K. Rai, R. K. Gupta, M. Martcheva, and A. K. Misra, "Modeling the control of bacterial disease by social media advertisements: Effects of awareness and sanitation," Journal of Biological Systems, vol. 30, no. 1, pp51-92, 2022.

[66] Q. Tong, X. Xu, and J. Zhang, "A fractional-order SEIDR network public opinion dissemination prediction model considering the heterogeneity of susceptibilities and dissuasion mechanism," IAENG International Journal of Applied Mathematics, vol. 54, no. 12, pp2766-2774, 2024.

[67] Q. Tong, S. Yue, J. Zhang, Y. Liu, and Z. Han, "A SEInIeR cyber public opinion propagation prediction model with extreme emotion mechanism," IAENG International Journal of Computer Science, vol. 51, no. 5, pp477-488, 2024.

[68] M. Turkyilmazoglu, "A highly accurate peak time formula of epidemic outbreak from the SIR model," Chinese Journal of Physics, vol. 84, pp39-50, 2023.

[69] B. Yang, Z. Yu, Y. Cai, "The impact of vaccination on the spread of COVID-19: Studying by a mathematical model," Physica A: Statistical Mechanics and its Applications, vol. 590, 2022, 126717.

[70] B. Yong, J. Hoseana, and L. Owen, "From pandemic to a new normal: Strategies to optimise governmental interventions in Indonesia based on an SVEIQHR-type mathematical model," Infectious Disease Modelling, vol. 7, no. 3, pp346-363, 2022.

[71] B. Yong, L. Owen, and J. Hoseana, "Mathematical analysis of an epidemic model for COVID-19: how important is the people's cautiousness level for eradication?," Letters in Biomathematics, vol. 9, no. 1, pp3-22, 2022.

[72] C. Zhai, P. Chen, Z. Jin, and T. K. Siu, "Epidemic modelling and actuarial applications for pandemic insurance: A case study of Victoria, Australia," Annals of Actuarial Science, vol. 18, no. 2, pp242-269, 2024.

[73] Z. Zhang and R. K. Upadhyay, "Dynamical analysis for a deterministic SVIRS epidemic model with Holling type II incidence rate and multiple delays," Results in Physics, vol. 24, 104181, 2021.

[74] J. Zhang, Z. Zhang, C. Zhou, and X. Ma, "A new SIQR model and residual power series method in wireless sensor networks," IAENG International Journal of Computer Science, vol. 51, no. 9, 1240-1249, 2024.

[75] Q. Zhu, L. Li, and C. Gan, "Modeling and analysis of the impact of adaptive defense strategy on virus spreading," IAENG International Journal of Applied Mathematics, vol. 48, no. 2, 146-151, 2018.